

$^{142}\text{Nd}(p, p')$ reaction on analog resonances*

L. Bimbot, † L. Lessard, † S. Santhanam, ‡ and R. Martin
*Laboratoire de Physique Nucléaire, Département de Physique,
 Université de Montréal, Montréal, Québec, Canada*

O. Dietzsch, § D. Spalding, ¶ and K. Schechet
University of Pittsburgh, Pittsburgh, Pennsylvania 15260

and

J. L. Foster, Jr., §
*Laboratoire de Physique Nucléaire, Département de Physique,
 Université de Montréal, Montréal, Québec, Canada
 and the University of Pittsburgh, Pittsburgh, Pennsylvania 15260*

(Received 17 August 1973)

The reaction ^{142}Nd has been measured on four analog resonances in the $^{142}\text{Nd} + p$ system at incident energies of 9.515, 10.250, 10.830, and 11.084 MeV. On each of the resonances spectroscopic factors are determined for those levels believed to have significant neutron particle-hole components.

[NUCLEAR REACTIONS $^{142}\text{Nd}(p, p')$, $E=9.5-11$ MeV on analog resonances, measured $\sigma(\Theta)$. ^{142}Nd deduced levels, J, π , spectroscopic factors. Enriched targets, Breit-Wigner analysis, resolution 5–15 keV, $\Theta = 20-170^\circ$.]

I. INTRODUCTION

The study of proton inelastic scattering through isobaric-analog resonances provides a valuable tool in the determination of nuclear structure.¹⁻⁶ Recently the inelastic decay of analog resonances has been extensively^{2, 3, 7-11} studied in the $N=82$ region. In this work we present the results of an investigation of the reaction $^{142}\text{Nd}(p, p')$ on four analog resonances^{12, 13} in the $^{142}\text{Nd} + p$ system, the parent states¹⁴ of which have a large single neutron component coupled to the ^{142}Nd ground-state core.

A previous high-resolution study¹⁵ (3 to 6 keV) with a magnetic spectrometer on the same resonances permitted the identification of a large number of levels in ^{142}Nd . Here additional measurements made with silicon detectors with a resolution of about 15 keV confirm absolute cross sections and complete the angular distributions, permitting a complete spectroscopic analysis. A similar study without detailed spectroscopic analysis was made by Muddersbach, Heusler, and Wurm¹⁶ on two of the four resonances with a resolution of 35 to 50 keV.

II. EXPERIMENTAL PROCEDURE

A. Silicon detector data

Targets of ^{142}Nd , isotopically enriched to 97.6%,

were bombarded by the proton beam of the Université de Montréal tandem Van de Graaff accelerator. The scattered particles were detected by an array of four surface-barrier detectors cooled to -15°C . Resolution was about 15 keV in each of the four detectors.

Angular distributions were taken in 10° steps from 70 to 170° on four analog resonances^{12, 13} in the $^{142}\text{Nd} + p$ system at laboratory energies of 9.515, 10.250, 10.830, and 11.084 MeV. The spins and parities of these resonances were determined to be $\frac{7}{2}^-$, $\frac{3}{2}^-$, $\frac{1}{2}^-$, and $\frac{5}{2}^-$ by Clausnitzer *et al.*¹³ through polarization measurements. An additional angular distribution was taken at 9.87 MeV in order to determine the off-resonance excitation of each state. The $\frac{7}{2}^-$ and $\frac{3}{2}^-$ resonances were located by taking excitation functions in 10-keV steps. The energy of the estimated maximum yield of the major noncollective levels was taken as the resonance energy. For the $\frac{1}{2}^-$ and $\frac{5}{2}^-$ resonances, the energy of the maximum yield of the 2^+ first excited state was taken as the resonance energy. Figure 1 shows the 130° spectra of the particle-hole region taken on each of the resonances. Figure 2 shows a complete off-resonance spectrum.

Absolute cross sections were determined from 4.0-MeV elastic scattering. The product of the solid angle subtended by a given detector and the target thickness is measured by assuming that at

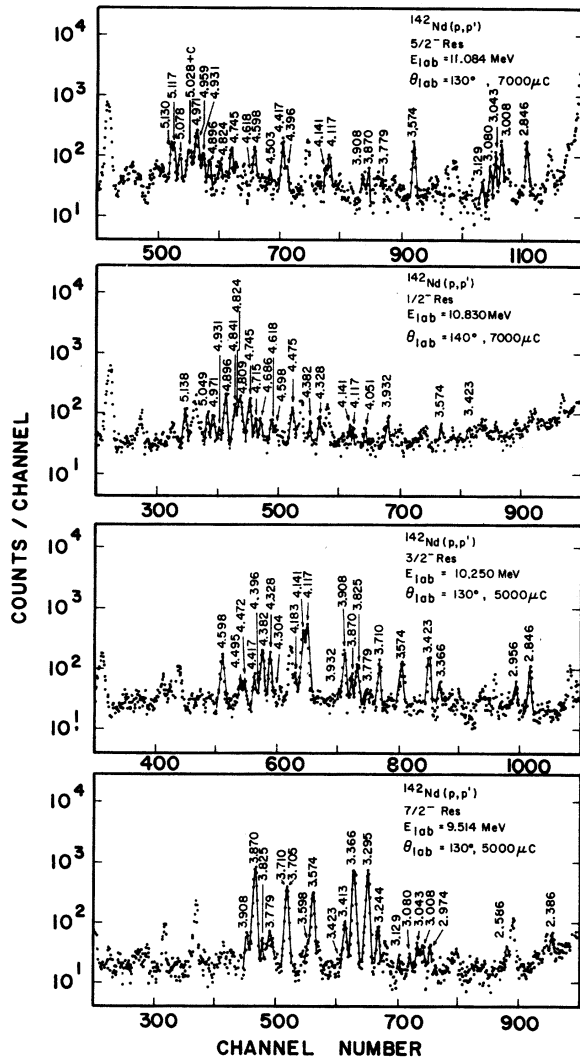


FIG. 1. Spectra at 130° on the $\frac{7}{2}^-$, $\frac{3}{2}^-$, $\frac{1}{2}^-$, and $\frac{5}{2}^-$ analog resonances in the neutron particle-hole region.

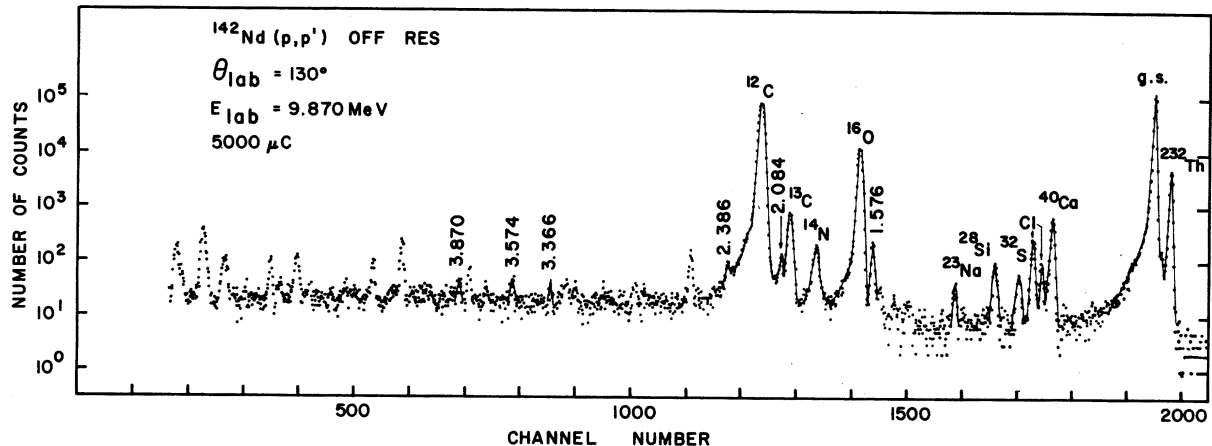


FIG. 2. Complete off-resonance spectrum.

TABLE I. Elastic scattering parameters averaged from measurements of Grosse *et al.* (Ref. 12) which are used in the present analysis. The resonance energies and single-particle widths are taken from this work.

| | $E_{c.m.}$ (MeV) | Γ_T (keV) | Γ_{p_0} (keV) | $\frac{1}{\Gamma_{sp}^{1/2}}$ (keV) | S_{pp_0} |
|-----------|---------------------|---------------------|-------------------------|--|------------|
| $f_{1/2}$ | 9.447 | 55 | 10.5 | 0.0785 | 0.82 |
| $p_{3/2}$ | 10.178 | 76 | 23.5 | 0.023 | 0.54 |
| $p_{1/2}$ | 10.754 | 74 | 22.7 | 0.021 | 0.48 |
| $f_{5/2}$ | 11.006 | 59 | 6.0 | 0.0395 | 0.24 |

4 MeV the elastic scattering of protons is purely Rutherford. The same target angle is then kept throughout the experiment. Absolute cross-section normalizations in this work are estimated to be accurate to $\pm 5\%$.

Target preparation presented special problems.¹⁷ A tungsten crucible containing a mixture of 6 mg Nd_2O_3 and 12 mg of thorium powder was heated through electron bombardment. Reduction into metallic form and evaporation of the neodymium occurred simultaneously. Targets were about $100 \mu\text{g}/\text{cm}^2$ Nd on $5\text{-}\mu\text{g}/\text{cm}^2$ carbon foils.¹⁸

B. Spectrograph data

This part of the experiment, carried out at the University of Pittsburgh, is well described in Ref. 15. Data was taken at 143, 120, 90, 70, 50, and 20° on the $\frac{7}{2}^-$ resonance; at 143, 120, 90, 70, 47, and 20° on the $\frac{3}{2}^-$ resonance; at 143 and 110° on the $\frac{1}{2}^-$ resonance; and at 143 and 120° on the $\frac{5}{2}^-$ resonance. The resonance energies were about 10 keV lower than those found for the counter data.

TABLE II. Optical-model parameters determined for the $^{142}\text{Nd}(p, p')$ analysis.

| r_c | V_0 (MeV) | r_0 (fm) | a (fm) | W_d (MeV) | r_i (fm) | a_i (fm) | V_{so} (MeV) | r_{so} (fm) | a_{so} (fm) |
|-------|----------------|---------------|-------------|----------------|---------------|---------------|-------------------|------------------|------------------|
| 1.25 | 54.6 | 1.25 | 0.65 | 11.9 | 1.25 | 0.47 | 6.2 | 1.25 | 0.65 |

The form of the optical potential is

$$U(r) = V_c - V_0 f(r, r_0, A^{1/3}, a) - iW_D a_i \frac{d}{dr} f(r, r_i, A^{1/3}, a_i) + \vec{\sigma} \cdot \vec{I} \left(\frac{\hbar}{m\pi c} \right)^2 \frac{V_{so}}{r} \frac{d}{dr} f(r, r_{so}, A^{1/3}, a_{so}),$$

where $f(r, r_0, A^{1/3}, a_0)$ is the usual Woods-Saxon form and r_c is the uniform sphere charge radius.

III. ANALYSIS

A. Inelastic scattering analysis

The inelastic angular distributions are analyzed using a Breit-Wigner expression. Neglecting any non-resonant contribution, the differential cross section for a spin-zero target is given by⁸

$$\frac{d\sigma}{d\Omega} = \frac{\chi^2 \Gamma_{p_0}}{2\Gamma_T^2} (2J_R + 1) \left(\frac{\Gamma_T^2/4}{(E - E_R)^2 + \Gamma_T^2/4} \right) (-1)^{2J_R - J_F} \sum_{\substack{\kappa=0,2,\dots \\ j_1 l_1, j_2 l_2}}^{\kappa_{\max}} \Gamma_{l_1 j_1}^{1/2} \Gamma_{l_2 j_2}^{1/2} A(L_R, J_R, K, l_1, j_1, l_2, j_2) \times \cos(\gamma_{l_1 j_1} - \gamma_{l_2 j_2}) P_K(\cos \theta), \quad (1)$$

where

$$A(L_R, J_R, K, l_1, j_1, l_2, j_2) = \overline{Z}(L_R, J_R, L_R, J_R, \frac{1}{2}K) \overline{Z}(l_1, j_1, l_2, j_2, \frac{1}{2}K) W(j_1, J_R, j_2, J_R, J_F, K).$$

The sum is over even K with

$$K_{\max} \leq \min[2L_R, 2J_R, \max(2l), \max(2j)]$$

and

$$|J_R - J_F| \leq j \leq |J_R + J_F|.$$

Here χ is the wave number of the incident proton and E is the incident energy; J_R and L_R are the spin and orbital angular momentum associated with the elastic resonance, E_R is the resonance

energy, Γ_{p_0} is the elastic partial width and Γ_T is the total width of the resonance; $\Gamma_{l_i j_i}$ is the inelastic width for the partial wave specified by orbital angular momentum l_i and total angular momentum j_i . The phase γ_{ij} is given by¹⁹

$$\gamma_{ij} = \omega_i + \xi_{ij} + \varphi_{ij}^R,$$

with ω_i , ξ_{ij} and φ_{ij}^R being, respectively, the Coulomb phase, the real part of the optical phase, and the resonance mixing phase. For our analysis we have taken $\varphi_{ij}^R = 0$.

Integration of Eq. (1) over a 4π solid angle gives the total cross section

$$\sigma = 2\pi\chi^2 \frac{\Gamma_{p_0}}{\Gamma_T^2} (2J_R + 1) \sum \Gamma_{l_j}$$

for $E = E_R$.

The quadratic nature of Eq. (1) assures there will be multiple solutions, only one of which can be the actual physical solution. Computer code GRILLE was written to determine the values of the partial widths which give the minimum χ^2 fits to the data using Eq. (1). In this program a grid search is made to hunt for minima and then a search routine is employed, using the grid minima as starting values.

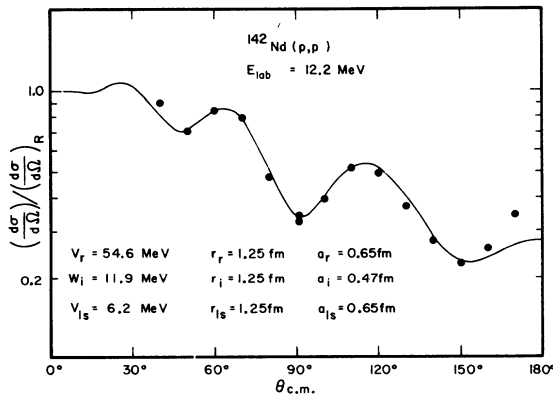


FIG. 3. Optical-model fit to $^{142}\text{Nd}(p, p)$ at 12.2 MeV laboratory energy.

The Γ_{p_0} and Γ_T used in the inelastic scattering analysis were taken from the elastic scattering measurements of Grosse *et al.*¹² The values used for the four resonances are shown in Table I.

B. Optical-model and single-particle widths

The optical phases used in the inelastic analysis depend upon the optical model used as do the single-particle widths. In order to precisely determine optical-model parameters a proton elastic angular distribution was taken at 12.2 MeV. At this proton energy the effect of the analog resonances should be negligible. Using code MAGALI²⁰

a fit was made to the data. Table II shows the optical parameters obtained. Figure 3 shows the fit. The real and imaginary well depths were allowed to vary while the geometric parameters were held constant at the values of Perey.²¹ The spin-orbit potential was arbitrarily fixed at 6.2 MeV.

With the optical potentials obtained from MAGALI, single-particle widths Γ_{sp}^{lj} were calculated by the method of Thompson, Adams, and Robson²² using program ANSPEC.²³ The same well geometry and spin-orbit potential is used for the bound neutron as is used for the real optical potential. It was found in Ref. 11 that large variations in well parameters produced only small variations in the

TABLE III. Total cross sections of highly excited levels observed in $^{142}\text{Nd}(p,p')$. The quantity σ_{nr} is 4π times the average backward-angle cross section at 9.87 MeV. In our notation 3.63 6 means 3.63 ± 0.06 .

| Energy (MeV) | Spin | $\sigma_{7/2-}$ 9.515 MeV (mb) | $\sigma_{3/2-}$ 10.250 MeV (mb) | $\sigma_{1/2-}$ 10.830 MeV (mb) | $\sigma_{5/2-}$ 11.080 MeV (mb) | σ_{nr} 9.870 MeV (mb) | Reasons for spin assignment |
|--------------|------------------------------------|--------------------------------------|---------------------------------------|---------------------------------------|---------------------------------------|------------------------------------|-----------------------------------|
| 3.244 | (4 ⁻) | 0.27 5 | | | | | a |
| 3.295 | 4 ⁻ , 3 ⁻ | 3.63 6 | | | | | b |
| 3.366 | 3 ⁻ , 4 ⁻ | 4.00 12 | 0.13 5 | | | 0.08 5 | c |
| 3.413 | (5 ⁻) | 0.44 5 | | | | | d |
| 3.423 | (1 ⁻) | 0.07 5 | 0.59 5 | 0.06 3 | | | e |
| 3.574 | (3 ⁻) | 1.50 7 | 0.47 3 | 0.10 3 | 0.55 10 | 0.14 5 | f |
| 3.598 | (5 ⁻) | 0.12 3 | | | | | d |
| 3.705 | (5 ⁻) | 0.83 3 | | | | | |
| 3.710 | (3 ⁻) | 1.06 6 | 0.47 3 | | | | g |
| 3.779 | (3 ⁻) | 0.13 3 | 0.12 3 | | 0.09 3 | | h |
| 3.825 | (2 ⁻) | 0.09 3 | 0.43 3 | | | | i |
| 3.870 | (4 ⁻) | 3.97 5 | 0.33 3 | | 0.11 3 | 0.06 5 | j |
| 3.908 | (2 ⁻) | 0.17 3 | 0.89 4 | | 0.12 5 | | k |
| 3.932 | | | 0.08 1 | 0.10 4 | 0.06 3 | | |
| 4.051 | | | | 0.06 3 | | | |
| 4.117 | 2 ⁻ , 1 ⁻ | | 2.85 10 | 0.10 4 | 0.20 3 | | l |
| 4.141 | 1 ⁻ , 2 ⁻ | | 2.22 5 | 0.05 3 | 0.14 3 | | |
| 4.183 | | | 0.12 3 | | | | |
| 4.304 | | | 0.07 3 | | | | |
| 4.328 | (1 ⁻ , 2 ⁻) | | 0.75 3 | 0.22 4 | | | m |
| 4.382 | (1 ⁻ , 2 ⁻) | | 0.39 3 | 0.13 4 | | | m |
| 4.396 | | | 0.13 3 | | 0.13 6 | | |
| 4.417 | (3 ⁻) | | 0.27 3 | | 0.40 5 | | n |
| 4.472 | | | 0.12 3 | | | | |
| 4.495 | (0 ⁻) | | 0.10 3 | 0.28 4 | | | o |
| 4.503 | | | | | 0.10 3 | | |
| 4.598 | (2 ⁻) | | 0.59 4 | | 0.34 4 | | p |
| 4.618 | | | | 0.12 4 | 0.07 3 | | |
| 4.686 | | | | 0.10 4 | | | |
| 4.715 | | | | 0.20 4 | | | |
| 4.745 | (1 ⁻ , 2 ⁻) | | | 0.47 6 | 0.38 6 | | q |
| 4.809 | (0 ⁻ , 1 ⁻) | | | 0.53 6 | | | r |
| 4.824 | (2 ⁻ , 1 ⁻) | | | 0.29 6 | 0.25 3 | | s |
| 4.841 | (0 ⁻) | | | 0.44 5 | | | r |
| 4.896 | (1 ⁻) | | | 0.63 6 | 0.17 5 | | t |
| 4.931 | (2 ⁻) | | | 0.08 3 | 0.32 5 | | u |
| 4.959 | (3 ⁻ , 2 ⁻) | | | | 0.28 6 | | v |

TABLE III (Continued)

| Energy (MeV) | Spin | $\sigma_{7/2^-}$ | $\sigma_{3/2^-}$ | $\sigma_{1/2^-}$ | $\sigma_{5/2^-}$ | σ_{nr} | Reasons for spin assignment |
|-----------------|------------------------------------|-------------------|--------------------|--------------------|--------------------|-------------------|-----------------------------------|
| | | 9.515 MeV (mb) | 10.250 MeV (mb) | 10.830 MeV (mb) | 11.080 MeV (mb) | 9.870 MeV (mb) | |
| 4.971 | (2 ⁻) | | | 0.08 3 | 0.98 9 | | u |
| 5.028 | | | | | 0.11 4 | | |
| 5.049 | | | | 0.04 2 | | | |
| 5.078 | | | | | 0.21 3 | | |
| 5.117 | (3 ⁻ , 2 ⁻) | | | | 0.28 5 | | v |
| 5.130 | (4 ⁻ , 3 ⁻) | | | | 0.40 4 | | w |
| 5.138 | (0 ⁻ , 1 ⁻) | | | 0.28 6 | | | r |
| 5.229 | | | | 0.16 5 | | | |

^a Angular distribution on $\frac{7}{2}^-$ resonance indicates 3⁻ or 4⁻. Seen only on $\frac{7}{2}^-$ resonance favors 4⁻.

^b Large $\sigma_{7/2^-}$ requires 3⁻ or 4⁻. Seen only $\frac{7}{2}^-$ resonance favors 4⁻.

^c Large $\sigma_{7/2^-}$ requires 3⁻ or 4⁻. Seen off resonance favors natural parity 3⁻.

^d Seen only on $\frac{7}{2}^-$ resonance. Correct angular distribution for 5⁻. No $l=0$ component in $^{143}\text{Nd}(d, t)$ distribution.

^e Large $\sigma_{3/2^-}$ indicates 1⁻ or 2⁻. Forward-peaked angular distribution on $\frac{7}{2}^-$ resonance suggests natural parity.

^f Angular distribution on $\frac{7}{2}^-$ resonance indicates 3⁻ or 4⁻. Resonant on $\frac{3}{2}^-$ indicates 3⁻. Seen off resonance favors natural parity as does forward-peaked angular distribution.

^g Angular distribution on $\frac{7}{2}^-$ resonance and large $\sigma_{7/2^-}$ indicate 3⁻ or 4⁻. Seen on $\frac{3}{2}^-$ resonance indicates 3⁻.

^h Seen on $\frac{7}{2}^-$, $\frac{3}{2}^-$, and $\frac{5}{2}^-$ resonances indicates 2⁻ or 3⁻. Angular distribution in $^{143}\text{Nd}(d, t)$ has $l=0$ component indicating 3⁻ or 4⁻.

ⁱ Seen on $\frac{7}{2}^-$ and $\frac{3}{2}^-$ resonances indicate 2⁻ or 3⁻. Angular distribution on $\frac{7}{2}^-$ resonance that of 2⁻. Angular distribution on $\frac{3}{2}^-$ resonance favors 1⁻ or 2⁻. No $l=0$ component in $^{143}\text{Nd}(d, t)$ angular distribution.

^j Large $\sigma_{7/2^-}$ requires 3⁻ or 4⁻. Believed to be 4⁻ on the basis of comparison with other $N=82$ nuclei (Refs. 3, 5, and 8).

^k Resonates on $\frac{7}{2}^-$, $\frac{3}{2}^-$, and $\frac{5}{2}^-$ resonances indicates 2⁻ or 3⁻. Form of angular distribution on $\frac{7}{2}^-$ resonance that of 2⁻. Form of angular distribution on $\frac{3}{2}^-$ resonance that of 1⁻ or 2⁻. No $l=0$ component in $^{143}\text{Nd}(d, t)$ angular distribution.

^l Large $\sigma_{3/2^-}$ requires 1⁻ or 2⁻ for both states. Comparison (Refs. 3, 5, and 8) with ^{140}Ce and other $N=82$ nuclei suggests 2⁻, 1⁻ order for spins. Identifying the doublet as the 1⁻ and 2⁻ members of the $\frac{3}{2}^- \otimes (d_{3/2})^{-1}$ multiplet, one obtains physically reasonable solutions only with the 2⁻, 1⁻ ordering.

^m Seen on $\frac{3}{2}^-$ and $\frac{1}{2}^-$ resonances indicates 0⁻, 1⁻, or 2⁻. $\sigma_{3/2^-}$ is too large for 0⁻. Not seen on $\frac{5}{2}^-$ resonance favors 1⁻.

ⁿ Form of angular distribution on $\frac{5}{2}^-$ resonance indicates 2⁻ or 3⁻. Not seen on $\frac{1}{2}^-$ resonance favors 3⁻. Form of angular distribution on $\frac{3}{2}^-$ resonance compatible with 3⁻.

^o Seen on $\frac{3}{2}^-$ and $\frac{1}{2}^-$ resonances indicates 0⁻, 1⁻, or 2⁻. Large $\sigma_{1/2^-}$ suggests 0⁻ or 1⁻. Form of angular distribution on $\frac{3}{2}^-$ resonance compatible with 0⁻. Not seen on $\frac{5}{2}^-$ resonance favors 0⁻.

^p Seen on $\frac{3}{2}^-$ and $\frac{5}{2}^-$ resonances indicates 1⁻, 2⁻, or 3⁻. Form of angular distribution on $\frac{3}{2}^-$ resonance that of 1⁻ or 2⁻. Form of angular distribution on $\frac{5}{2}^-$ resonance that of 2⁻ or 3⁻.

^q Seen on $\frac{1}{2}^-$ and $\frac{5}{2}^-$ resonances indicates 1⁻ or 2⁻. Large $\sigma_{1/2^-}$ suggests 0⁻ or 1⁻. Angular distribution on $\frac{5}{2}^-$ resonance compatible with 1⁻.

^r Seen on $\frac{1}{2}^-$ resonance indicates 0⁻, 1⁻, or 2⁻. Not seen on $\frac{5}{2}^-$ resonance suggests not 2⁻ and favors 0⁻.

^s Seen on $\frac{1}{2}^-$ and $\frac{5}{2}^-$ resonances indicates 1⁻ or 2⁻. Angular distribution on $\frac{5}{2}^-$ resonance compatible with any spin.

^t Seen on $\frac{1}{2}^-$ and $\frac{5}{2}^-$ resonances indicates 1⁻ or 2⁻. Large $\sigma_{1/2^-}$ suggests 0⁻ or 1⁻. Angular distribution on $\frac{5}{2}^-$ resonance compatible all allowed spins.

^u Seen on $\frac{1}{2}^-$ and $\frac{5}{2}^-$ resonances indicates 1⁻ or 2⁻. Angular distribution on $\frac{5}{2}^-$ resonance that of 2⁻ or 3⁻.

^v Seen on $\frac{3}{2}^-$ resonance indicates 1⁻, 2⁻, 3⁻, or 4⁻. Not seen on $\frac{1}{2}^-$ resonance suggests 3⁻ or 4⁻. Angular distribution that of 2⁻ or 3⁻.

^w Large $\sigma_{5/2^-}$ eliminates 1⁻ and indicates 2⁻, 3⁻, or 4⁻. Not seen on $\frac{1}{2}^-$ resonance suggests 3⁻ or 4⁻. Angular distribution compatible with 4⁻.

TABLE IV. Resonant off-parity states in $^{142}\text{Nd}(p, p')$ on the 9.514-MeV I_2^- resonance.

| E_x (MeV) | $\Gamma_{sp}^{-1}(\frac{3}{2})$ (keV) $^{-1}$ | $\Gamma_{sp}^{-1}(\frac{1}{2})$ (keV) $^{-1}$ | Probable solution | | | Other solutions | | | | | | | | |
|----------------|--|--|-------------------|----------------------------|----------------------------|-------------------|------------------------|--------------------|-----------------|----------------------------|----------------------------|-------------------|--------------------|--------------------|
| | | | J_{π}^{\pm} | $\Gamma(d_{3/2})$ (keV) | $\Gamma(s_{1/2})$ (keV) | Relative phase | $S_{pp'}(\frac{3}{2})$ | $S_{pp'}(s_{1/2})$ | J_{π}^{\pm} | $\Gamma(d_{3/2})$ (keV) | $\Gamma(s_{1/2})$ (keV) | Relative phase | $S_{pp'}(d_{3/2})$ | $S_{pp'}(s_{1/2})$ |
| 3.24 | 1.10 | 0.232 | 4 $^-$ | 0.038 | 0.035 | ... | 0.04 | 0.01 | 4 $^-$ | 0.070 | 0.002 | ... | 0.07 | 0.00 |
| 3.295 | 1.20 | 0.252 | 4 $^-$ | 0.424 | 0.528 | ... | 0.45 | 0.12 | 4 $^-$ | 0.944 | 0.007 | ... | 1.00 | 0.00 |
| 3.366 | 1.35 | 0.283 | 3 $^-$ | 0.336 | 0.710 | + | 0.52 | 0.23 | 3 $^-$ | 0.372 | 0.581 | + | 0.51 | 0.17 |
| 3.413 | 1.54 | 0.310 | 5 $^-$ | 0.111 | | | 0.12 | | 3 $^-$ | 0.748 | 0.205 | + | 1.03 | 0.06 |
| 3.574 | 2.00 | 0.410 | 3 $^-$ | 0.002 | 0.352 | ... | 0.01 | 0.16 | 3 $^-$ | 0.880 | 0.166 | + | 1.35 | 0.05 |
| 3.598 | 2.10 | 0.450 | 5 $^-$ | 0.027 | | | 0.05 | | 4 $^-$ | 0.406 | 0.641 | ... | 0.49 | 0.16 |
| 3.705 | 2.66 | 0.525 | 5 $^-$ | 0.212 | | | 0.41 | | 4 $^-$ | 1.046 | 0.001 | ... | 1.26 | 0.00 |
| 3.710 | 2.68 | 0.535 | 3 $^-$ | 0.0001 | 0.243 | ... | 0.00 | 0.15 | 3 $^-$ | 0.234 | 0.001 | ... | 0.72 | 0.00 |
| 3.779 | 3.00 | 0.590 | 3 $^-$ | 0.002 | 0.026 | ... | 0.01 | 0.02 | 3 $^-$ | 0.023 | 0.008 | ... | | |
| 3.825 | 3.30 | 0.650 | 2 $^-$ | 0.024 | | | 0.13 | | 4 $^-$ | 0.770 | 0.254 | + | 2.49 | 0.16 |
| 3.870 | 3.65 | 0.700 | 4 $^-$ | 0.011 | 1.01 | ... | 0.03 | 0.63 | | | | | | |
| 3.908 | 3.82 | 0.770 | 2 $^-$ | 0.043 | | | 0.26 | | | | | | | |

TABLE V. Resonant odd-parity states in $^{142}\text{Nd}(p, p')$ on the 10.250-MeV I_2^- resonance.

| E_x (MeV) | $\Gamma_{sp}^{-1}(d_{3/2})$ (keV) $^{-1}$ | $\Gamma_{sp}^{-1}(s_{1/2})$ (keV) $^{-1}$ | Probable solution | | | Other solutions | | | | | | | | |
|----------------|--|--|-------------------|----------------------------|----------------------------|-------------------|--------------------|--------------------|-----------------|----------------------------|----------------------------|-------------------|--------------------|--------------------|
| | | | J_{π}^{\pm} | $\Gamma(d_{3/2})$ (keV) | $\Gamma(s_{1/2})$ (keV) | Relative phase | $S_{pp'}(d_{3/2})$ | $S_{pp'}(s_{1/2})$ | J_{π}^{\pm} | $\Gamma(d_{3/2})$ (keV) | $\Gamma(s_{1/2})$ (keV) | Relative phase | $S_{pp'}(d_{3/2})$ | $S_{pp'}(s_{1/2})$ |
| 3.423 | 0.455 | 0.104 | 1 $^-$ | 0.024 | 0.232 | + | 0.03 | 0.03 | 1 $^-$ | 0.250 | 0.006 | + | 0.15 | 0. |
| 3.574 | 0.575 | 0.127 | 3 $^-$ | 0.269 | | | 0.09 | | | | | | | |
| 3.710 | 0.720 | 0.157 | 3 $^-$ | 0.266 | | | 0.11 | | | | | | | |
| 3.779 | 0.805 | 0.172 | 3 $^-$ | 0.056 | | | 0.05 | | | | | | | |
| 3.825 | 0.860 | 0.184 | 2 $^-$ | 0.006 | 0.195 | ... | 0.01 | 0.03 | 2 $^-$ | 0.131 | 0.070 | + | 0.09 | 0.01 |
| 3.908 | 0.990 | 0.212 | 2 $^-$ | 0.056 | 0.370 | ... | 0.04 | 0.06 | 2 $^-$ | 0.351 | 0.074 | + | 0.28 | 0.01 |
| 4.117 | 1.400 | 0.298 | 2 $^-$ | 0.174 | 1.091 | + | 0.20 | 0.26 | 2 $^-$ | 1.058 | 0.207 | + | 1.18 | 0.05 |
| 4.141 | 1.470 | 0.314 | 1 $^-$ | 0.215 | 0.877 | ... | 0.42 | 0.37 | 1 $^-$ | 1.087 | 0.178 | + | 2.03 | 0.07 |
| 4.328 | 2.100 | 0.431 | 1 $^-$ | 0.076 | 0.263 | ... | 0.21 | 0.15 | 1 $^-$ | 0.068 | 1.198 | + | 0.13 | 0.48 |
| 4.382 | 2.320 | 0.475 | 2 $^-$ | 0.025 | 0.148 | ... | 0.08 | 0.09 | 2 $^-$ | 0.732 | 0.359 | + | 1.43 | 0.15 |
| 4.417 | 2.500 | 0.505 | 3 $^-$ | 0.129 | | | 0.18 | | 2 $^-$ | 1.059 | 0.032 | + | 1.24 | 0.00 |
| 4.495 | 2.870 | 0.580 | 0 $^-$ | 0.046 | | | 0.53 | | 2 $^-$ | 0.371 | 0.720 | ... | 0.43 | 0.18 |
| 4.598 | 3.600 | 0.700 | 2 $^-$ | 0.011 | 0.286 | ... | 0.03 | 0.16 | 1 $^-$ | 0.301 | 0.038 | ... | 0.84 | 0.02 |
| | | | | | | | | | 1 $^-$ | 0.032 | 0.150 | ... | 0.10 | 0.10 |
| | | | | | | | | | 1 $^-$ | 0.168 | 0.014 | ... | 0.52 | 0.01 |
| | | | | | | | | | 2 $^-$ | 0.204 | 0.093 | + | 0.59 | 0.05 |

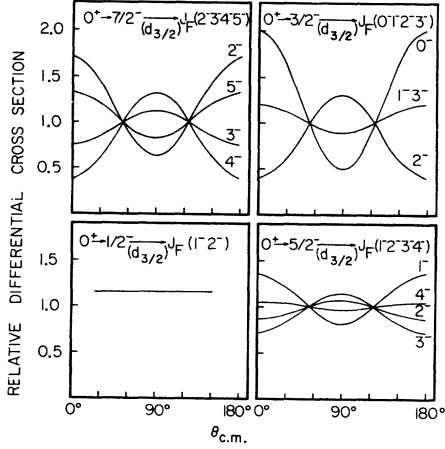


FIG. 4. Angular distributions for particle-hole states with a pure $d_{3/2}$ hole configuration on the four analog resonances studied.

Γ_{sp}^{ij} , provided the depths of the potentials were changed to give a good optical-model fit.

C. General considerations

In ^{142}Nd the 51 to 82 neutron shell is closed with occupied $2d_{3/2}$, $3s_{1/2}$, $1h_{11/2}$, $1g_{7/2}$, and $2d_{5/2}$ neutron subshells. The $2d_{3/2}$ and $3s_{1/2}$ energies are at the Fermi surface, while the $1h_{11/2}$, $1g_{7/2}$, and $2d_{5/2}$ neutron single-particle energies are from 1 to 2 MeV below.^{24, 25} In the next shell there are vacant $2f_{7/2}$, $3p_{3/2}$, $1h_{9/2}$, $3p_{1/2}$, $2f_{5/2}$, and $1i_{13/2}$ neutron subshells. The 10 protons above the closed 50 proton shell²⁶ occupy principally the $2d_{5/2}$ and $1g_{7/2}$ subshells with the $1h_{11/2}$, $3s_{1/2}$, and $2d_{3/2}$ proton subshells being essentially empty.

The wave function of a state in the $^{142}\text{Nd} + \text{neutron}$ system (a parent state) may be written⁵ as

$$\Psi_J = \alpha(n_J \otimes \Phi_0) + \sum_{ik} \beta_{ik}(n_i \otimes \Phi_k^*)_J, \quad (2)$$

where Φ_0 represents the ground state and the Φ_k^* are excited states of ^{142}Nd . The n_J and the n_i refer to neutrons in the otherwise empty $2f_{7/2}$, $2p_{3/2}$, $1h_{9/2}$, $2f_{5/2}$, and $1i_{13/2}$ subshells. The analog of this state is^{5, 6}

$$\begin{aligned} T^- \Psi_J &= \frac{\alpha}{(2T_0+1)^{1/2}} (p_J \otimes \Phi_0) && \text{term I} \\ &+ \alpha \left(\frac{2T_0}{2T_0+1} \right)^{1/2} (n_J \otimes T^- \Phi_0) && \text{term II} \\ &+ \sum_{jk} \frac{\beta_{jk}}{(2T_0+1)^{1/2}} (p_j \otimes \Phi_k^*)_J && \text{term III} \\ &+ \sum_{jk} \frac{\beta_{ik}}{(2T_0+1)^{1/2}} (n_j \otimes T^- \Phi_k^*)_J, && \text{term VI} \end{aligned} \quad (3)$$

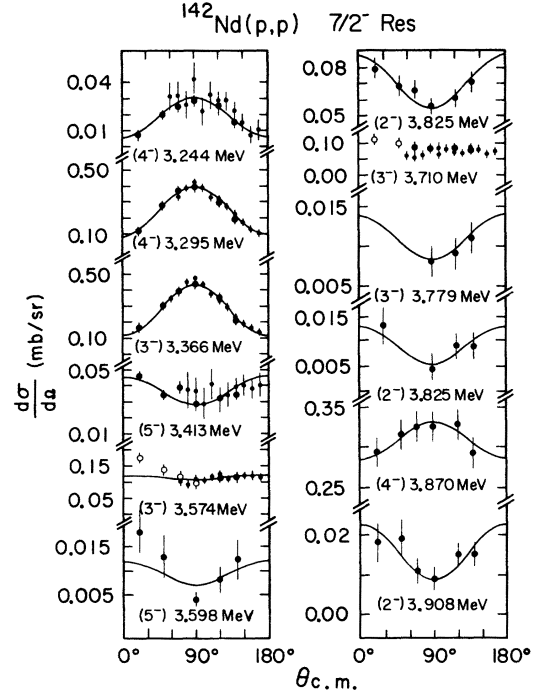


FIG. 5. Angular distributions and fits to the strongly resonant negative-parity levels on the $\frac{7}{2}^-$ analog resonance. The larger points represent spectrograph data; the smaller points are counter data. Open data points were not fitted.

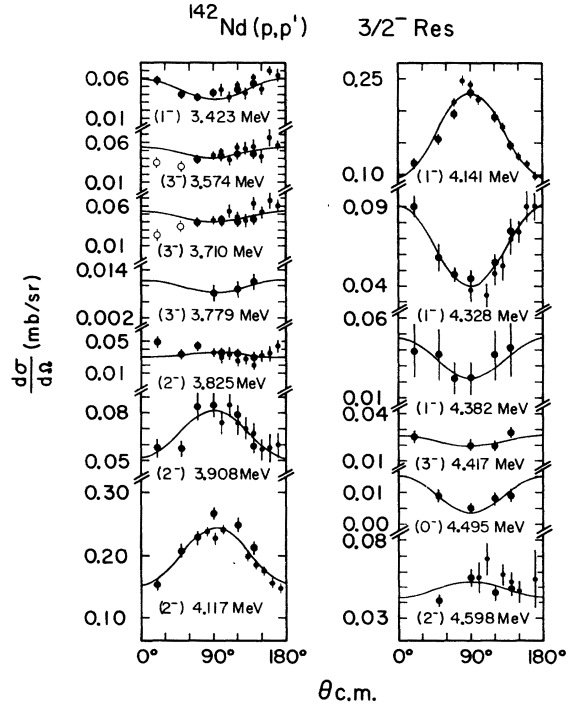


FIG. 6. Angular distributions and fits to the strongly resonant negative-parity states on the $\frac{3}{2}^-$ analog resonance. The conventions are those of Fig. 4.

where

$$T^{-}\Phi_0 = [1/(2T_0)^{1/2}] \sum_i (p_i)(n_i)^{-1} \Phi_0$$

and

$$T^{-}\Phi_k = [1/(2T_0)^{1/2}] \sum_i (p_i)(n_i)^{-1} \Phi_k.$$

Elastic scattering through the analog resonance occurs by absorption and emission of proton p_j in term I of Eq. (3). Decay of the analog state by emission of a charge-exchanged proton from term II will leave the residual nucleus in a neutron particle-hole configuration. Those excited states of the target nucleus Φ_k^* coupled to a neutron in the parent state will be populated by decay of protons from term III. Neutron particle-hole configurations based on excited target states should result from the emission of charge-exchanged protons from term IV in the same fashion as from term II.

The parent states of the resonances investigated in this experiment, with spins of $\frac{7}{2}^-$, $\frac{3}{2}^-$, $\frac{1}{2}^-$, and $\frac{5}{2}^-$, have a large component of a $2f_{7/2}$, $3p_{3/2}$, $3p_{1/2}$, or $2f_{5/2}$ neutron coupled to the ^{142}Nd ground state. The observed (p, p') spectra are dominated by states having a component of a $2f_{7/2}$, $3p_{3/2}$, $3p_{1/2}$, or $2f_{5/2}$ neutron (depending on the resonance) with a $2d_{3/2}$ or $3s_{1/2}$ neutron hole coupled to the ^{142}Nd ground state. Only $d_{3/2}$ and $s_{1/2}$ holes should be created in the final nucleus: $h_{11/2}$ and $g_{7/2}$ protons are prevented from leaving the nucleus by penetrability considerations and neutron-hole formation in $2d_{5/2}$ and $1g_{7/2}$ subshells is largely prevented by the proton subshells being already oc-

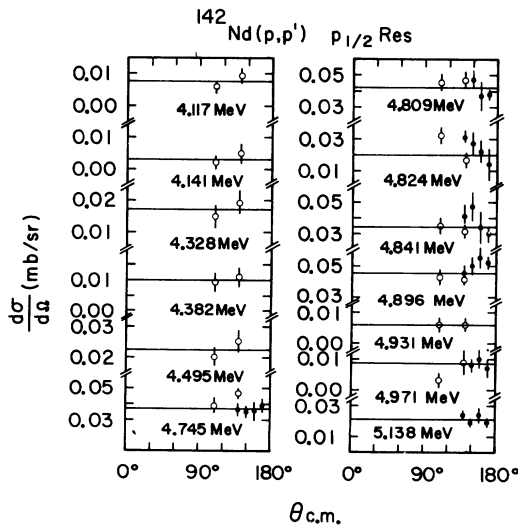


FIG. 7. Angular distributions and fits to the strongly resonant negative-parity levels on the $\frac{1}{2}^-$ analog resonance. The conventions are those of Fig. 4.

cupied. Table 2 in Ref. 15 shows the particle-hole multiplets one expects to see on the various resonances with spins, parities, and anticipated centroid energies calculated from $^{142}\text{Nd}(d, t)$ and $^{142}\text{Nd}(d, p)$ Q values. These states are all well above 3 MeV excitation. Low-lying levels which will involve mainly excited proton configurations can be strongly excited only because of neutron coupling to these states in the parent system (term III decay).

D. Spectroscopic factors and sum rules

For those states, Φ_k^* , of the target nucleus with no excited neutron components the spectroscopic factor is given by

$$S_{pp'} = \frac{\Gamma^{lj}}{\Gamma_{sp}^{lj}} = |\langle (n_j \otimes \Phi_k^*)_J | \Psi_{J_R} \rangle|^2 = \beta_{jk}^2, \quad (4)$$

where Ψ_{J_R} is the parent state and lj refers to neutron orbital j . This corresponds to term III decay. One has the sum rule

$$\alpha^2 + \sum_{jk} \beta_{jk}^2 = S_{pp0} + \sum S_{pp'} = 1.$$

For particle-hole final states, assuming a closed

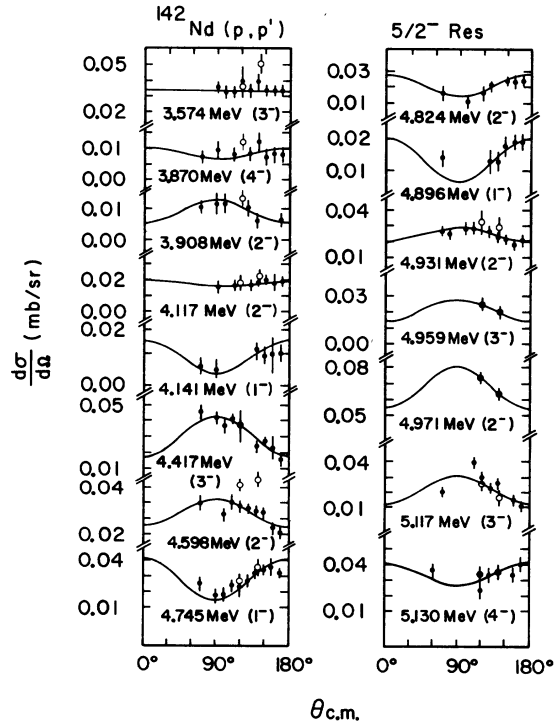


FIG. 8. Angular distributions and fits to the strongly resonant negative-parity levels on the $\frac{5}{2}^-$ analog resonance. The conventions are those of Fig. 4.

neutron shell, the spectroscopic factor⁸ is

$$S_{J_R}^{J_F}(lj) = \left(\frac{2J_R + 1}{2J_F + 1} \right) \frac{\Gamma^{lj}}{\Gamma_{sp}^{lj}} = |\langle \Phi_F | (n_i^{-1} \otimes \Psi_{J_R})_{J_F} \rangle|^2.$$

For the particle-hole states, $S_{J_R}^{J_F}(lj)$ is a measure of the parent state plus neutron-hole component of a final state, not of the shell-model configuration. On a given resonance, summing over all states of a given J_F one should find

$$\sum S_{J_R}^{J_F}(lj) = 1$$

for any hole orbital (lj). For a given level, summing over the available holes and over the different resonances studied

$$\sum_{\substack{lj \\ J_R}} S_{J_R}^{J_F}(lj) \leq 1.$$

E. Spin assignments

Only the spins of a few low-lying levels are known. In order to carry out an analysis, the spin of any state considered must be specified. While unambiguous spin assignments cannot be made on the basis of information obtained from this experiment, it is possible to limit the spin possibilities and to determine a most probable spin for the major peaks.

Table III shows the levels observed above 3.2 MeV excitation (probable particle-hole states) with the total cross section on each resonance deter-

mined from a Legendre polynomial fit of the angular distributions. Off resonance, 4π times the average backward-angle differential cross section gives a quantity σ_r , which can be compared with the on-resonance total cross sections. For the major levels the probable spin or spins are shown with an explanation. When more than one spin is given, that underlines is believed to be the more probable. Parentheses indicate lack of certainty.

In the inelastic proton channel we expect only $s_{1/2}$ and $d_{3/2}$ protons for the particle-hole region. States with pure $d_{3/2}$ protons for the particle-hole region. States with pure $d_{3/2}$ hole configurations will have angular distributions characteristic of their spin. Figure 4 shows these angular distributions for the four resonances studied. For pure $s_{1/2}$ hole configurations the angular distributions will be isotropic. Because of configuration mixing, only states with $J_F = J_R \pm \frac{3}{2}$ will have the characteristic angular distributions. The form of the angular distributions for states with $J_F = J_R \pm \frac{1}{2}$ will not be unique since there can, and in general will be, both $s_{1/2}$ and $d_{3/2}$ protons with interfering amplitudes in the exit channel. For a state to have a spin $J_F = J_R \pm \frac{3}{2}$ it is a necessary condition that it have the pure $d_{3/2}$ angular distribution. It is not a sufficient condition since states with $J_F = J_R \pm \frac{1}{2}$ can have almost any angular distribution because of interference between $s_{1/2}$ and $d_{3/2}$ amplitudes. Since in the particle-hole region $\Gamma_{sp}(s_{1/2}) \approx 5\Gamma_{sp}(d_{3/2})$, information can also be deduced from

TABLE VI. Strongly resonant states on the 11.084-MeV $\frac{1}{2}^-$ analog resonance. Since the angular distributions are isotropic, only the sum $\sum S_{p,p'}$ can be extracted; the individual partial widths cannot be.

| E_x (MeV) | J_F^π | $E_{c.m.}$ (keV) | $\Gamma_{sp}^{-1}(d_{3/2})$ (keV ⁻¹) | $\Gamma_{sp}^{-1}(s_{1/2})$ (keV ⁻¹) | $\sum \Gamma_{p,p'}$ (keV) | $S_{p,p'}(d_{3/2})$ | $S_{p,p'}(s_{1/2})$ |
|----------------|-------------------|---------------------|---|---|-------------------------------|---------------------|---------------------|
| 4.117 | (2 ⁻) | 6.637 | 0.55 | 0.123 | 0.10 | 0.02 | |
| | (1 ⁻) | | | | | ≤0.02 | ≤0.01 |
| 4.141 | (1 ⁻) | 6.613 | 0.57 | 0.126 | 0.05 | | |
| | (2 ⁻) | | | | | 0.01 | |
| 4.328 | (1 ⁻) | 6.426 | 0.77 | 0.165 | 0.22 | ≤0.11 | ≤0.02 |
| 4.382 | (1 ⁻) | 6.372 | 0.84 | 0.177 | 0.13 | ≤0.07 | ≤0.02 |
| | (2 ⁻) | | | | | 0.04 | |
| 4.495 | (0 ⁻) | 6.259 | 1.00 | 0.212 | 0.28 | ≤0.56 | ≤0.12 |
| 4.745 | (1 ⁻) | 6.009 | 1.35 | 0.325 | 0.47 | ≤0.42 | ≤0.10 |
| 4.809 | (0 ⁻) | 5.945 | 1.75 | 0.370 | 0.53 | ≤1.85 | ≤0.39 |
| 4.824 | (2 ⁻) | 5.930 | 1.77 | 0.375 | 0.29 | 0.20 | |
| | (1 ⁻) | | | | | ≤0.34 | ≤0.07 |
| 4.841 | (0 ⁻) | 5.913 | 1.82 | 0.385 | 0.44 | ≤1.60 | ≤0.33 |
| 4.896 | (1 ⁻) | 5.858 | 2.04 | 0.425 | 0.63 | ≤0.86 | ≤0.18 |
| 4.931 | (2 ⁻) | 5.823 | 2.20 | 0.455 | 0.08 | 0.07 | |
| 4.971 | (2 ⁻) | 5.783 | 2.40 | 0.485 | 0.08 | 0.08 | |
| 5.138 | (0 ⁻) | 5.616 | 3.40 | 0.660 | 0.28 | ≤1.90 | ≤0.37 |
| | (1 ⁻) | | | | | ≤0.63 | ≤0.12 |

TABLE VII. Resonant odd-parity states seen in $^{140}\text{Nd}(p,p')$ on 11.080-MeV $\frac{5}{2}^-$ resonance.

| E_x (MeV) | $\Gamma_{\text{sp}}^{-1}(d_{3/2})$ (keV) $^{-1}$ | $\Gamma_{\text{sp}}^{-1}(s_{1/2})$ (keV) $^{-1}$ | J_{F}^{π} | $\Gamma(d_{3/2})$ (keV) | $\Gamma(s_{1/2})$ (keV) | Probable solution | | | Other solutions | | | | |
|----------------|---|---|----------------------|----------------------------|----------------------------|---------------------|---------------------|----------------------|----------------------------|----------------------------|-------------------|---------------------|---------------------|
| | | | | | | $S_{p,p'}(d_{3/2})$ | $S_{p,p'}(s_{1/2})$ | J_{F}^{π} | $\Gamma(d_{3/2})$ (keV) | $\Gamma(s_{1/2})$ (keV) | Relative phase | $S_{p,p'}(d_{3/2})$ | $S_{p,p'}(s_{1/2})$ |
| 3.574 | 0.170 | 0.047 | 3 $^-$ | 0.19 | 0.15 | 0.03 | 0.01 | 0.00 | 0.34 | 0.00 | + | 0.00 | 0.01 |
| 3.870 | 0.258 | 0.065 | 4 $^-$ | 0.08 | 0.01 | 0.01 | | | | | | | |
| 3.908 | 0.270 | 0.068 | 2 $^-$ | 0.09 | 0.01 | 0.03 | 0.00 | 0.02 | 0.08 | 0.01 | + | 0.01 | 0.01 |
| 4.117 | 0.370 | 0.087 | 2 $^-$ | 0.16 | 0.01 | 0.08 | 0.00 | 0.00 | 0.17 | 0.00 | ... | 0.00 | 0.02 |
| 4.141 | 0.382 | 0.089 | 1 $^-$ | 0.08 | | 0.06 | | | | 0.14 | | 0.10 | |
| 4.417 | 0.590 | 0.131 | 3 $^-$ | 0.33 | 0.01 | 0.16 | 0.00 | 0.09 | 0.25 | 0.00 | ... | 0.06 | 0.00 |
| 4.598 | 0.790 | 0.170 | 2 $^-$ | 0.25 | 0.02 | 0.24 | 0.00 | 0.03 | 0.24 | 0.05 | + | 0.03 | 0.03 |
| 4.745 | 1.000 | 0.213 | 1 $^-$ | 0.23 | | 0.46 | | 0.03 | 0.23 | 0.05 | ... | 0.04 | 0.06 |
| 4.824 | 1.140 | 0.240 | 2 $^-$ | 0.04 | 0.13 | 0.06 | 0.04 | 0.21 | 0.04 | 0.01 | ... | 6.25 | 0.01 |
| 4.896 | 1.300 | 0.273 | 1 $^-$ | 0.12 | | 0.31 | | 0.11 | 0.06 | 0.02 | ... | 0.15 | 0.02 |
| 4.931 | 1.380 | 0.290 | 2 $^-$ | 0.01 | 0.25 | 0.02 | 0.09 | 0.25 | 0.00 | 0.41 | + | 0.41 | 0.00 |
| 4.959 | 1.460 | 0.300 | 3 $^-$ | 0.5 | 0.68 | 0.06 | 0.17 | 0.61 | 0.13 | 0.76 | + | 0.76 | 0.03 |
| 4.971 | 1.490 | 0.312 | 2 $^-$ | 0.05 | 0.22 | 0.08 | 0.29 | 0.23 | 0.01 | 1.29 | + | 1.29 | 0.00 |
| 5.117 | 1.920 | 0.405 | 3 $^-$ | 0.07 | 0.18 | 0.10 | 0.06 | 0.00 | 0.77 | 0.00 | ... | 0.00 | 0.21 |
| | | | | | | | | 0.76 | 0.02 | 0.97 | ... | 0.97 | 0.01 |
| | | | | | | | | 0.22 | 0.02 | 0.36 | + | 0.36 | 0.00 |
| | | | | | | | | 0.04 | 0.20 | 0.09 | + | 0.09 | 0.10 |
| | | | | | | | | 0.21 | 0.03 | 0.48 | + | 0.48 | 0.01 |
| 5.130 | 2.000 | 0.415 | 4 $^-$ | 0.31 | | 0.53 | | 0.01 | 0.31 | 0.02 | + | 0.02 | 0.11 |
| | | | | | | | | 0.12 | 0.19 | 0.21 | + | 0.21 | 0.07 |

cross sections. A large nonresonant cross section should favor a natural parity assignment (0^+ , 1^- , 2^+ , 3^- , 4^+ , etc.).

F. Results

Figures 5–8 show the angular distributions and fits to the strongly resonant states on the $\frac{7}{2}^-$, $\frac{3}{2}^-$, $\frac{1}{2}^-$, and $\frac{5}{2}^-$ resonances. Tables IV–VII show the partial widths obtained in the fitting procedure and the corresponding spectroscopic factors.

For those particle-hole states with both $s_{1/2}$ and $d_{3/2}$ hole components, Eq. (1) will have two different solutions for $\Gamma_{s_{1/2}}^{1/2}$ and $\Gamma_{d_{3/2}}^{1/2}$. If one of the solutions gives spectroscopic factors in excess of unity that solution may be rejected; otherwise we do not know which is the correct physical solution. On the $\frac{7}{2}^-$ analog resonance the 3^- and 4^- states will have both $d_{3/2}$ and $s_{1/2}$ neutron-hole components. The 3.295- and 3.366-MeV 4^- and 3^- levels each have only one solution with $S_{pp} < 1$. For other 3^- or 4^- states, that solution which appears more nearly orthogonal to the 3.366- or 3.295-MeV levels on the basis of the limited information available, is taken as the more probable. This is not a strictly valid criteria since we lack knowledge of a large portion of every wave function. On the $\frac{3}{2}^-$ resonance we take that solution for 1^- or 2^- states which is more nearly orthogonal to the 4.117- or 4.141-MeV levels as the most probable solution.

On the $\frac{5}{2}^-$ analog resonance there are no 2^- or 3^- states with sufficient spectroscopic strength for an orthogonality test to be meaningful. Below the particle-hole region the solution containing the largest $d_{3/2}$ hole component is energetically favored and has been arbitrarily taken, while in the particle-hole region we have taken that solution with the largest $s_{1/2}$ neutron-hole component. We assume the particle-hole region to begin with the 4.824-MeV state for the $\frac{5}{2}^-$ resonance.

The only apparently clear case of a $d_{5/2}$ hole component is the 3.870-MeV 4^- level. If this is

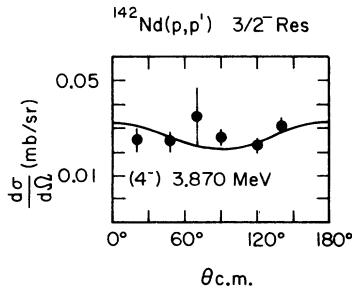


FIG. 9. Angular distribution and fit to 3.870-MeV level on $\frac{3}{2}^-$ analog resonance.

the state seen on the $\frac{3}{2}^-$ resonance (and not a very close-by neighbor), it is almost certainly due to a $\frac{3}{2}^-(d_{5/2})^{-1}$ component. Figure 9 shows the angular distribution and fit. Table VIII shows the results of the analysis, corrected for the $d_{5/2}$ proton occupancy.

IV. DISCUSSION AND INTERPRETATION

A. Spectroscopic strengths

Table IX shows the sums of the spectroscopic strength observed on the $\frac{7}{2}^-$, $\frac{3}{2}^-$, and $\frac{5}{2}^-$ resonances. On the $\frac{7}{2}^-$ resonance we are able to account for 50% of the $d_{3/2}$ and $s_{1/2}$ neutron-hole strength. On the $\frac{3}{2}^-$ resonance we find about the same situation though there is somewhat more fragmentation of the levels. The inelastic cross sections are smaller on the $\frac{1}{2}^-$ resonance because of the factor $(2J_R + 1)$ in Eq. (1) and on the $\frac{5}{2}^-$ resonance because of the reduced $f_{5/2}$ single-particle strength. The major resonant states on the $\frac{5}{2}^-$ resonance still contain half of the $d_{3/2}$ hole strength but only about a third of the $s_{1/2}$ neutron-hole strength. No systematic study was possible on the $\frac{1}{2}^-$ resonance.

On the $\frac{7}{2}^-$ and $\frac{3}{2}^-$ resonances between 40 and 70% of the wave functions of the individual states with large cross sections in the particle-hole region are accounted for by our simple model. On the $\frac{1}{2}^-$ and $\frac{5}{2}^-$ resonances from 30 to 50% of the individual wave functions of the major states are found if our spin assignments are correct.

A recent study connected with this work has shown (d, t) spectroscopic factors to be closely related to those obtained in (p, p') through analog resonances.²⁷

B. Level scheme

Figure 10 shows the levels of ^{142}Nd observed in our (p, p') studies¹⁵ together with the expected energies of low-lying neutron particle-hole multiplets and the calculated energies²⁸ of the members of the negative-parity quintuplet, $J^\pi = 1^-$ to 5^- ,

TABLE VIII. A probable $d_{5/2}$ hole component seen on the $\frac{3}{2}^-$ resonance.

$$S_{pp'}(j) = \frac{S(j)}{V_j^\pi},$$

where V_j^π ($2j + 1$) is the proton occupancy of the subshell j .

| E_x (MeV) | $E_{c.m.}$ (MeV) | $\Gamma_{sp}^{-1}(d_{5/2})$ (keV) ⁻¹ | $\Gamma(d_{5/2})$ (keV) | $S_{pp'}(d_{5/2})$ | $S_{pp'}(d_{5/2})$ |
|----------------|---------------------|--|----------------------------|--------------------|--------------------|
| 3.870 | 6.232 | 0.93 | 0.15 | 0.14 | 0.21 |

formed by coupling the 2^+ one-quadrupole phonon to the 3^- one-octupole phonon.

Though there is considerable configuration mixing, the principal components of the members of the $\frac{7}{2}^- \otimes (d_{3/2})^{-1}$ and $\frac{7}{2}^- \otimes (s_{1/2})^{-1}$ neutron particle-hole multiplets can be identified on the $\frac{7}{2}^-$ resonance. On the $\frac{3}{2}^-$ resonance the situation is less clear since except for the 4.495-MeV (0^-) level, no single hole component clearly dominates the wave function of any state. Still if one compares the spectra on the $\frac{7}{2}^-$ and $\frac{3}{2}^-$ resonances one sees definite correlations.

The 3.244-MeV (4^-) and 3.423-MeV (1^-) states are possibly the 1^- and 4^- members of the two-phonon quintet, there being in the vicinity no other

states identified as having these spins which are not principal members of particle-hole multiplets. There are several candidates for the 2^- , 3^- , and 5^- members of the quintet and the strength is probably shared among several states.

Through configuration mixing, the majority of low-spin negative-parity levels up to 5 MeV should be observed in this work.

ACKNOWLEDGMENTS

We are grateful to Professor Pierre Depommier and Professor B. L. Cohen for their support and encouragement of this work. We acknowledge helpful conversations with Professor Rory Coker.

*Work supported by the National Research Council of Canada and the U. S. National Science Foundation.

†Present address: Institut de Physique Nucléaire, Orsay, France.

‡Consultant.

§Present address: Instituto de Fisica, Universidade de Sao Paulo, Sao Paulo, Brazil.

¶Present address: Analytic Services Corporation, Falls Church, Virginia.

¹C. F. Moore, L. J. Parish, P. von Brentano, and S. A. A. Zaidi, *Phys. Lett.* **22**, 616 (1966).

²G. C. Morrison, N. Williams, J. A. Nolen, Jr., and D. von Ehrenstein, *Phys. Rev. Lett.* **19**, 592 (1967).

³P. A. Moore, P. J. Riley, C. M. Jones, M. D. Mancusi and J. L. Foster, Jr., *Phys. Rev. C* **1**, 1100 (1970); *Phys. Rev. Lett.* **22**, 356 (1969).

⁴C. F. Moore, S. A. A. Zaidi, and J. J. Kent, *Phys. Rev. Lett.* **18**, 345 (1967).

⁵G. C. Morrison, in *Nuclear Isospin*, edited by J. D. Anderson, S. D. Bloom, J. Cerny, and W. W. True (Academic, New York, 1970), p. 435.

⁶N. Stein, in *Nuclear Isospin* (see Ref. 5), p. 451.

⁷P. J. Wurm, A. Heusler, and P. von Brentano, *Nucl. Phys.* **A128**, 433 (1969).

⁸A. Heusler, H. L. Harney, and J. P. Wurm, *Nucl. Phys.* **A135**, 591 (1969).

⁹A. Heusler, *Nucl. Phys.* **A141**, 667 (1970).

¹⁰H. L. Hiddleston and P. J. Riley, *Phys. Lett.* **32B**, 423 (1970).

¹¹R. Martin, L. Bimbot, L. Lessard, S. Gales, D. Spalding, W. G. Weitkamp, O. Dietzsch and J. L. Foster, Jr. *Nucl. Phys.* **A210**, 221 (1973).

¹²E. Grosse, K. Melchoir, H. Seitz, P. von Brentano,

J. P. Wurm, and S. A. A. Zaidi, *Nucl. Phys.* **A142**, 345 (1970).

¹³G. Clausnitzer, R. Fleischman, G. Graw, D. Proetel, and J. P. Wurm, *Nucl. Phys.* **A106**, 99 (1968).

¹⁴C. A. Wiedner, A. Heusler, J. Solf, and J. P. Wurm, *Nucl. Phys.* **A103**, 433 (1967).

¹⁵S. Raman, J. L. Foster, Jr., O. Dietzsch, D. Spalding, and B. H. Wildenthal, *Nucl. Phys.* **A201**, 21 (1973).

¹⁶K. Muddersbach, A. Heusler, and J. P. Wurm, *Nucl. Phys.* **A146**, 477 (1970).

¹⁷L. Westgaard and S. Bjornholm, *Nucl. Instrum.* **42**, 77 (1966).

¹⁸Yissum Research Development Corporation, Jerusalem, Israel.

¹⁹W. J. Thompson, in *Nuclear Isospin* (see Ref. 5), p. 427.

²⁰R. Raynal, Centre d'Etudes Nucléaire, Saclay, France, Internal Report MAGALI (unpublished).

²¹F. G. Perey, *Phys. Rev.* **132**, 755 (1963).

²²W. J. Thompson, J. L. Adams, and D. Robson, *Phys. Rev.* **173**, 975 (1968).

²³W. J. Thompson and J. L. Adams, Tandem Accelerator Laboratory, Florida State University, Tallahassee, Florida, Technical Report ANSPEC (unpublished).

²⁴R. K. Jolly and E. Kashy, *Phys. Rev. C* **4**, 887, 1398 (1971).

²⁵A. Chaumeaux, G. Brugge, H. Faraggi, and J. Picard, *Nucl. Phys. C* **4**, 176 (1971).

²⁶B. H. Wildenthal, E. Newman, and R. L. Auble, *Phys. Lett.* **27B**, 628 (1968); *Phys. Rev. C* **3**, 1199 (1971).

²⁷J. L. Foster, Jr., O. Dietzsch, and L. Bimbot, *Phys. Rev. Lett.* **31**, 731 (1973).

²⁸P. Vogel and L. Kocbach, *Nucl. Phys.* **A176**, 33 (1971).